Exosomes from PYCR1 knockdown bone marrow mesenchymal stem inhibits aerobic glycolysis and the growth of bladder cancer cells via regulation of the EGFR/PI3K/AKT pathway

ZHUO LI, YING JIANG, JIAN LIU, HUIFENG FU, QUAN YANG, WEI SONG and YUANWEI LI

Department of Urology, Hunan Provincial People's Hospital, The First Affiliated Hospital of
Hunan Normal University, Changsha, Hunan 410002, P.R. China

Abstract. Bladder cancer (BC) is a heterogeneous disease, and pyrroline-5-carboxylate reductase 1 (PYCR1) can promote the proliferation and invasion of BC cells and accelerate BC progression. In the present study, si-PYCR1 was loaded into bone marrow mesenchymal stem cell (BMSC)-derived exosomes (Exos) in BC. First, PYCR1 levels in BC tissues/cells were assessed, and cell proliferation, invasion, and migration were evaluated. Aerobic glycolysis levels (glucose uptake, lactate production, ATP production, and the expression of relevant enzymes) and the EGFR/PI3K/AKT pathway phosphorylation levels were determined. PYCR1-EGFR interactions were examined by co-immunoprecipitation experiments. RT4 cells transfected with oe-PYCR1 were treated with EGFR inhibitor CL-387785. Exos were loaded with si-PYCR1 and identified, followed by an assessment of their effects on aerobic glycolysis and malignant cell behaviors. Nude mouse models of xenograft tumors were established by injecting mice with Exo-si-PYCR1 and Exo-si-PYCR1. PYCR1 was upregulated in BC cells, with the highest expression observed in T24 cells and the lowest expression in RT4 cells. Following PYCR1 knockdown, the malignant behaviors of T24 cells and aerobic glycolysis were decreased, while PYCR1 overexpression in RT4 cells averted these trends. PYCR1 interacted with EGFR, and CL-387785 inhibited the EGFR/PI3K/AKT pathway and attenuated the effects of PYCR1 overexpression on RT4 cells but had no effect on PYCR1 expression. Exo-si-PYCR1 showed stronger inhibitory effects on aerobic glycolysis and on the malignant behaviors of T24 cells than si-PYCR1. Exo-si-PYCR1 blocked xenograft tumor growth and had good biocompatibility. Briefly,

Correspondence to: Dr Yuanwei Li, Department of Urology, Hunan Provincial People's Hospital, The First Affiliated Hospital of Hunan Normal University, 61 Jiefang West Road, Furong, Changsha, Hunan 410002, P.R. China
Email: liyuanwei_8@163.com

PYCR1 knocking loaded by BMSC-derived Exos suppressed aerobic glycolysis and BC growth via the PI3K/AKT pathway by binding to EGFR.

Introduction

Bladder cancer (BC) is one of the most common types of cancer worldwide and the most prevalent malignancy of the urinary tract (1). BC accounts for ~200,000 deaths and 500,000 newly diagnosed cases worldwide (2). Apart from age and geography, the risk varies between sexes and is notably affected by exposure to various carcinogens, with cigarette smoke being the most common (1). Until recently, treatment for BC, for several years, was limited to surgery and chemotherapy or immunotherapy (3). Although these therapies have certain beneficial effects in the initial stages of treatment, BC patients are prone to relapse and metastasis in the later stages, leading to treatment failure and patient death (4). Therefore, it is of great significance to search for more effective molecular-targeted therapies for BC.

Pyrroline-5-carboxylate reductase 1 (PYCR1) is a major enzyme involved in proline production in the mitochondria, which not only participates in the metabolism of amino acids but is also associated with energy metabolism and mitochondrial function and plays a pivotal role in cell proliferation and apoptosis (5,6). A previous study demonstrated the potential role of PYCR1 in facilitating the progression of BC, and PYCR1 may be utilized as a promising and attractive anticancer target for BC therapy (7). The transformation from mitochondrial oxidative phosphorylation to aerobic glycolysis in metabolism is called the Warburg effect, and the cancer progression attributed to aerobic glycolysis is often related to the activation of oncogenes or the loss of tumor suppressor genes (8). Aerobic glycolysis is a scientifically identified hallmark of the metabolism of cancer cells and targeting it may provide possible drug-target cancer therapy strategies (9). Aerobic glycolysis participates in the proliferation, migration, and invasion of hepatocellular carcinoma (HCC) cells (10). EGFR is a tyrosine kinase receptor that functions in the pathways controlling aberrant and normal cell growth (11). EGFR expression is dysregulated in various types of tumors, such as melanoma, colorectal cancer, non-small cell lung cancer, and breast cancer (12-15). The PI3K/AKT pathway is frequently

activated in human cancers, inducing cell malignant transformation and tumor angiogenesis and apoptosis (16). The EGFR/PI3K/AKT pathway stimulates aerobic glycolysis of cancer cells by regulating the key enzymes of aerobic glycolysis, glucose transporter type 1 (GLUT1) (17,18). The PI3K/AKT axis is also correlated with PYCR1 expression, and the mRNA levels of AKT1 and PIK3CB are positively related to PYCR1 in gastric cancer tissues (19). However, whether PYCR1 regulates the EGFR/PI3K/AKT pathway and aerobic glycolysis in BC remains unknown. Small interfering RNAs (siRNAs) are widely used to knock down the posttranscriptional expression of genes through complementarity to mRNAs in the cytoplasm (20). Various polymer-based nonviral gene vectors have been designed to deliver siRNAs into the cytoplasm in an efficient manner due to the tailored advantages of polymeric biomaterials, and siRNAs have potential as cancer therapeutics (21-23). Exosomes (Exos) are the smallest type of extracellular vesicles (40-100 nm in diameter), consisting of a lipid bilayer surface structure and containing various essential biomolecules including DNA, lipid, protein, and RNA, acting as indispensable cell communication mediators (24). Exos have the characteristics of good biocompatibility and low toxicity and immunogenicity and play significant roles in the development and metastasis of cancers (25,26). Therefore, delivery of siRNAs targeting PYCR1 (si-PYCR1) through Exos for BC treatment may theoretically be of clinical value. However, there are no reports, to the best of our knowledge, on the mechanism of bone marrow mesenchymal stem cell (BMSC)-derived Exos (BMSC-Exos) with PYCR1 expression knocked down on the aerobic glycolysis and growth of BC cells. The aim of this study was to elucidate the mechanism of PYCR1 in BC and to establish a therapeutic modality using BMSC-Exos vector containing si-PYCR1 for the management of BC, serving as a reference for elucidating the pathogenesis of BC and developing novel targeted therapies for the management of BC.

Materials and methods

Ethics statement. All procedures were authorized by the Academic Ethics Committee of Hunan Provincial People's Hospital, The First Affiliated Hospital of Hunan Normal University (approval no. 2021-071) and were strictly implemented in accordance with the National Laboratory Animal Guide (27). Laboratory procedures were performed in such a manner as to reduce the pain and discomfort caused to mice. The need for approval for the use of primary human BMSCs was waived by the Ethics Committee of Hunan Provincial People's Hospital, The First Affiliated Hospital of Hunan Normal University.

Database analysis of PCYR1 expression in BC. The StarBase database (starbase.sysu.edu.cn/panCancer.ph) was used to determine PCYR1 expression in BC as follows: Select 'Gene Differential Expression', search 'PCYR1 (ENSG00000183010)', and select 'Bladder Urothelial Carcinoma'. The results were downloaded from the database.

Cell culture. Normal bladder epithelial cell SV-HUC-1 and BC cell lines T24, 5637, RT4, and TCCSUP (ATCC) were cultured in the RPMI-1640 medium (all from Gibco; Thermo Fisher Scientific, Inc.) supplemented with 10% FBS, 100 U/ml penicillin, and 100 μg/ml streptomycin in a humidified incubator (Eppendorf) supplied with 5% CO_2 air at 37°C. Cells in the logarithmic growth phase were collected and PCYR1 levels in cells were determined by reverse transcription-quantitative polymerase chain reaction (RT-qPCR) and western blotting.

Extraction of BMSC-Exos. Human BMSCs (cat. no. 7500, ScienCell Research Laboratories, Inc.) were cultured and subcultured according to the manufacturer's instructions. After 5 subcultures, Exos in the BMSC supernatant culture medium were extracted by ultracentrifugation. BMSCs were cultured to 60% confluence, and the medium was replaced with Exo-free serum (EXO-FBS-50A-1, SBI). When the cell density reached 85%, the supernatant was centrifuged at 4°C at 2,000 g for 15 min. The collected supernatant was then centrifuged at 4°C at 16,500 g for 30 min, filtered with 0.22-μm filter membranes to remove particles >200 nm, and centrifuged twice at 4°C at 100,000 g for 70 min, and the Exos in the lower layer were collected, resuspended in 100 μl PBS, and stored at -80°C. The supernatant of BMSCs treated with GW4869, an inhibitor of exosome secretion (10 μM, cat. no. HY-19363, MedChemExpress), for 24 h was used as the negative control (NC) of Exos (28).

Preparation of Exo-si-PYCR1 using the electroporation method. Cy3-si-PYCR1 (orange fluorescent label) was synthesized by Shanghai GenePharma Co., Ltd. The extracted Exos and Cy3-si-PYCR1 were added to the electroporation cuvettes (Bio-Rad Laboratories, Inc., Gene Pulser Xcell electroporation system) at the mass ratio of 5:1 (500 ng:100 ng) and were electroplated for 2 sec at 400 V and 125 μF. Subsequently, the mixture was centrifuged at 135,000 g and 4°C for 70 min to obtain Exo-si-PYCR1, resuspended in 100 μl PBS and stored at -80°C.

Identification of Exos and Exo-si-PYCR1. The morphological structure of Exos and Exo-si-PYCR1 was observed using a transmission electron microscope (TEM) (FEI). The particle size distribution and ζ potential of Exos and Exo-si-PYCR1 were measured using a Malvern Laser Particle Sizer (DLS, Zetasizer Nano ZS90, Malvern Instruments). The positive expression of surface marker proteins CD9, CD81, CD63, and TSG101 (Abcam) in Exos and Exo-si-PYCR1 was detected by western blotting. The content changes of free si-PYCR1 in Exos, free si-PYCR1, and Exo-si-PYCR1 after electroporation were determined by agarose gel electrophoresis to determine whether si-PYCR1 was loaded into Exos.

Observation of Exo-si-PYCR1 uptake by BC cells using laser confocal microscopy. T24 cells ($2x10^5$) were seeded in the confocal Petri dishes and used for the control group, si-PYCR1 group, and Exo-si-PYCR1 group. The control cells were not treated, cells in the si-PYCR1 group were transfected with free Cy3-si-PYCR1 (100 ng) using Lipofectamine® 2000 reagent (cat. no. 11668-019; Invitrogen; Thermo Fisher Scientific, Inc.), and cells in the Exo-si-PYCR1 group were transfected with Exo-si-PYCR1 with Cy3-si-PYCR1 (100 ng). After 24 h of transfection, cells were incubated with immunostaining

fixative (cat. no. P0098, Beyotime Institute of Biotechnology) for 10 min and washed with immunostaining detergent (cat. no. P0106, Beyotime Institute of Biotechnology) for 5 min x 4 times. Then, to the confocal Petri dishes, 200 μl green-fluorescent probe was added (Actin-Tracker Green, cat. no. C1033, Beyotime Institute of Biotechnology) diluted with immunofluorescence staining secondary antibody diluent (1:200, cat. no. P0108, Beyotime Institute of Biotechnology) and incubated at 37˚C for 30 min. After staining, the cells were washed with detergent for 5 min x 4 times, incubated with DAPI working solution for 10 min, and washed with PBS 4 times; the uptake rate (%) of Cy3-si-PYCR1 by T24 cells was observed under a laser confocal microscope (magnification, x200, Leica GmbH).

Cell grouping and treatment. T24 cells and RT4 cells were seeded in 6-well plates, cultured until 80% confluence, and divided into the following groups based on different treatments: i) blank group, T24 cells or RT4 cells normally cultured for 48 h; ii) si-PYCR1 group and si-NC group, T24 cells transfected with the si-PYCR1 or the NC, respectively; iii) oe-PYCR1 group and oe-NC group, RT4 cells transfected with the oe-PYCR1 or the NC, respectively; iv) oe-PYCR1 + Vehicle group and oe-PYCR1 + CL-387785 group, RT4 cells treated with EGFR inhibitor CL-387785 (1 μM, cat. no. HY-10325, MedChemExpress) or solvent (0.1% DMSO) for 2 h and transfected with oe-PYCR1. The dosage and method of use of CL-387785 were determined according prior to the study (data not shown); v) Exo group, T24 cells were cultured with Exos (100 ng/well) for 48 h; and vi) Exo-si-NC group and Exo-si-PYCR1 group, T24 cells were cultured with Exo-si-NC or Exo-si-PYCR1 (containing si-NC or si-PYCR1 100 ng/well) for 48 h. si-PYCR1, oe-PYCR1, and corresponding NCs used in transfection were synthesized by Shanghai GenePharma CO., Ltd. The sequences of si-RNAs were: si-PYCR1 forward, 5'-UGCUAUCAACGCUGUGG-3' and reverse, 5'-CCACAG CGUUGAUAGCA-3'; and si-NC forward, 5'-AAUUCUCCG AACGUGUACGU-3' reverse, 5'-ACGUACACGUUCGGA GAAUU-3'. pcDNA3.1 was used as the vector of oe-PYCR1, and oe-NC corresponded to the empty plasmid. After 48 h of transfection, PYCR1 levels were determined by RT-qPCR and western blotting.

MTT assay. Cell viability was detected using an MTT assay. Briefly, 2,000 T24 or RT4 cells were seeded in 96-well plates. After 48 h of culture, cells were incubated with 20 μl MTT solution (0.5%, cat. no. M1025, Beijing Solarbio Science & Technology Co., Ltd.) at 37˚C for 4 h, and then MTT solution was removed. Next, 100 μl DMSO was added to cells, and the plates were shaken at a constant speed for 10 min to fully dissolve the formazan crystals. The optical density value at 490 nm was measured using a microplate reader (Thermo Fisher Scientific, Inc.).

Transwell assays. After 48 h of transfection, the cells in each group were collected and made into cell suspensions. The invasive ability of BC cells was assessed using Transwell chambers (cat. no. 3413, Corning, Inc.). Matrigel matrix adhesive was spread (60 μl, Corning) on the bottom of the apical chamber, 100 μl cell suspension was added to the chamber, with a cell count of approximately 1×10^5, and 700 μl RPMI-1640 medium comprising 10% fetal bovine serum was added to the basolateral chamber. Following 48 h of incubation, the non-invasive cells in the apical chamber of the Transwell chamber were wiped off with a cotton swab, cells were fixed with 4% paraformaldehyde at 37˚C for 30 min, and stained with 0.1% crystal violet at 37˚C for 10 min. The number of cells passing through the membrane pores was observed under a microscope (200x, Olympus Corporation) in three random fields for each well; the number of invasive cells in the different groups was counted.

Wound-healing assay. The migratory ability of BC cells was assessed using a wound-healing assay. After 48 h of transfection, T24 or RT4 cells were seeded at 5×10^4 cells/well in 96-well plates and cultured in an. Once a confluent monolayer had formed, a scratch was created using a 200-μl sterile pipette gun head by vertically marking a line under an inverted microscope (Olympus Corporation) and imaged at 0 and 24 h. The cell migration rate (%) was calculated by measuring the width of the wound.

Determination of glucose uptake, lactate, and ATP production levels. The levels of aerobic glycolysis-related indicators, glucose uptake, lactate production, and ATP production were determined using the colorimetric method. The glucose uptake colorimetric assay kit (cat. no. 36503, AAT Bioquest), lactate detection kit (cat. no. KTB1100-1, Abbkine Scientific Co., Ltd.), and ATP detection kit (cat. no. YT6278, Beijing YITA Biotechnology) were used according to the instructions of the kits.

Co-immunoprecipitation (Co-IP). T24 cells in the exponential phase were collected and total protein was extract using weak RIPA lysate (P0013D, Beyotime, Shanghai, China), and protein concentration was determined using BCA reagent kit (P0012, Beyotime). The 200 μg of total protein was taken and 1 μg PYCR1 antibody (cat. no. ab102601, Abcam) was added and incubated overnight at 4˚C. Then, 10 μl pre-treated protein A (cat. no. YJ101, Epizyme Biomedical Technology) agarose bead was added to the solution and incubated for 2 h at 4˚C to allow coupling of the antibody with protein A agarose bead. Following immunoprecipitation, the mixture was centrifuged for 3 min at 4˚C and 200 x g to sink the agarose bead to the bottom of the tube. The supernatant was removed carefully, and the agarose bead was washed 3 times with 1 ml lysis buffer before examining the binding of PYCR1 and EGFR protein using western blotting. IgG antibody (cat. no. ab6715, Abcam) was used as a negative control, and protein lysis buffer without immunoprecipitation was used as a positive control (Input).

Xenograft tumor models. The 6-week-old male BALB/c nude mice (Cavens Laboratory Animal) were used to establish the xenograft tumor model. T24 cells have a high tumor formation rate in nude mice. T24 cells in the logarithmic growth phase were detached into a single-cell suspension and subcutaneously injected into the armpits of mice (2×10^6 cells per mouse). Drug intervention was performed when the subcutaneous tumor grew to ~100 mm^3 (tumor volume=long x width^2 x 1/2). The mice with tumor formations were randomly assigned to

one of four groups (n=6 per group): NC group, BMSC-Exo group, BMSC-Exo-si-NC group, and BMSC-Exo-si-PYCR group, in which mice were administered 200 μl normal saline, BMSC-Exo, BMSC-Exo-si-NC, and BMSC-Exo-si-PYCR1, respectively, by tail vein injection on days 0, 3, 6, and 9, respectively. The physical conditions and behavior of mice were observed daily during the medication period. The weight of mice was measured on days 0, 2, 4, 6, 8, and 12, respectively. The volume of the xenografted tumor was measured once a week. The tumor volume was measured for the last time in the 5th week (the 35th day) (maximum tumor long diameter: 15.0 mm). Then, mice were euthanized by intraperitoneal injection of 1% pentobarbital sodium (200 mg/kg). The tumors were removed for observation and imaging, weight measurement, and immunohistochemical staining.

RT-qPCR. BC cells or tumor tissues of nude mice were collected. Total RNA was extracted using the TRIzol® reagent (cat. no. 15596018; Invitrogen; Thermo Fisher Scientific, Inc.) and reverse transcribed into cDNA using the RNA RT kit according to the manufacturer's protocol (cat. no. 4387406; Invitrogen; Thermo Fisher Scientific, Inc.). qPCR was performed using the ABI Prism 7300 system using the following amplification temperature protocol: Pre-denaturation, 95°C for 30 sec; followed by 40 cycles of denaturation at 95°C for 5 sec, annealing at 60°C for 30 sec, and extension at 72°C for 30 sec. The relative gene expression was analyzed using the $2^{-\Delta\Delta Cq}$ method (29), with β-Actin as the internal reference control. The primers were synthesized by Sangon Biotech Co., Ltd. The sequences were as follows: PYCR1:F: 5'-GGCTGCCCA CAAGATAATGGC-3'; R: 5'-CAATGGAGCTGATGGTGA CGC-3' and β-actin: F: 5'-AATGAGCTGCGTGTGGCT-3'; R: 5'-TAGCACAGCCTGGATAGCAA-3'.

Western blotting. Cells were collected and lysed using RIPA lysis buffer (cat. no. P0013B, Beyotime Institute of Biotechnology) to obtain total proteins from cells or tumor tissues of nude mice. Protein concentration was determined using a BCA kit. Equal amounts of proteins protein were loaded on SDS-gels, resolved using 10% SDS-PAGE, and transferred to PVDF membranes. Membranes were blocked with 5% skimmed milk for 1 h and incubated overnight with the following antibodies: PYCR1 (1:1,000, cat. no. ab102601; Abcam), GLUT1 (1 μg/ml, cat. no. ab115730, Abcam), hexokinase 1 (HK1; 1:1,000, cat. no. ab154839, Abcam), lactic dehydrogenase A (LDHA; 1:5.000, ab52488, Abcam), EGFR (1:10.000, ab52894, Abcam), p-EGFR (1:1,000, ab40815, Abcam), PI3K (1:1,000, ab32089, Abcam), p-PI3K (0.5 μg/ml, ab278545, Abcam), AKT (1:500, ab8805, Abcam), p-AKT (1:1,000, ab38449, Abcam), and β-Actin (1:1,000, ab8227, Abcam). After incubation with the primary antibodies, the membranes were probed with horseradish peroxidase-conjugated secondary antibody (1:3,000, ab6721, Abcam) for 1 h. Finally, Signals were visualized using the ChemiDoc MP Imaging System (Bio-Rad Laboratories, Inc.).

Immunohistochemical staining. Tumor tissues were fixed with 4% paraformaldehyde at 4°C for 24 h and cut into 5-μm thick paraffin-embedded sections. As previously reported (30), the sections were routinely dewaxed and hydrated, and subjected to antigen retrieval using sodium citrate buffer (pH=6.0) in a microwave oven at 100°C for 10 min and incubated with 3% H_2O_2 at room temperature for 10 min to block the activity of endogenous peroxidase. After washing with PBS, the sections were incubated with the primary antibody against Ki-67 (1:250, cat. no. ab92742, Abcam) in the dark at 4°C overnight. After PBS washes, the sections were incubated at room temperature with the secondary antibody goat anti-rabbit IgG H&L HRP (1:500, cat. no. ab97051, Abcam) for 30 min at 37°C, washed with PBS, counterstained with hematoxylin for 30 sec at 37°C, differentiated with 0.1% HCl, rinsed with tap water to return to blue for 5 min. Subsequently, the sections were dehydrated with a gradient of alcohol solutions, cleared with xylene, and sealed with neutral gum. After air drying, the sections were observed and imaged under a light microscope (x200, Olympus Corporation).

Biosafety investigation. The safety of Exo-si-PYCR1 was investigated by observing the weight changes of mice in each group during the drug intervention period (days 0-12). After mice were euthanized by intraperitoneal injection of 1% pentobarbital sodium (200 mg/kg), the major organs (heart, liver, spleen, lung, and kidney) of mice were collected for pathological HE staining to further investigate the effects of Exo-si-PYCR1 on these organs.

Statistical analysis. GraphPad Prism version 8.01 (GraphPad Software Inc.) was used to perform the statistical analysis. A Shapiro-Wilk test was used to evaluate the distribution of data. *In vitro* experiments were performed three times in each group, and 6 nude mice were included in each group for the *in vivo* experiments. The normally distributed data are presented as the mean ± SD. An independent samples Student's t-test was used for comparisons between 2 groups and a one-way ANOVA followed by Tukey's post hoc test was used to compare differences between multiple groups. P<0.05 was considered to indicate a statistically significant difference. a statistically significant difference.

Results

PYCR1 expression is upregulated in BC cells and it promotes cell growth. PYCR1 expression is upregulated in various types of cancer and it is involved in the regulation of BC cell behaviors (31,32). Using the StarBase database, it was found that PYCR1 levels were upregulated in BC (Fig. 1A, P<0.05). Next, PYCR1 levels in SV-HUC-1 normal human bladder epithelial immortalized cells and four BC cells (T24, 5637, RT4, and TCCSUP) were determined by RT-qPCR and western blot assay. PYCR1 was found to be upregulated in the four BC cell lines, in which T24 cells exhibited the highest level and RT4 cells exhibited the lowest levels (Fig. 1B and C, all P<0.05). To investigate the effects of PYCR1 on BC cells, interference plasmids were transfected into T24 cells to knock down PYCR1, and overexpression plasmids were transfected into RT4 cells to increase PYCR1 levels. RT-qPCR and western blot assays showed that PYCR1 was successfully knocked down in T24 cells and overexpressed in RT4 cells (Fig. 1D and E, all P<0.001). MTT assay showed that T24 cell viability was decreased following
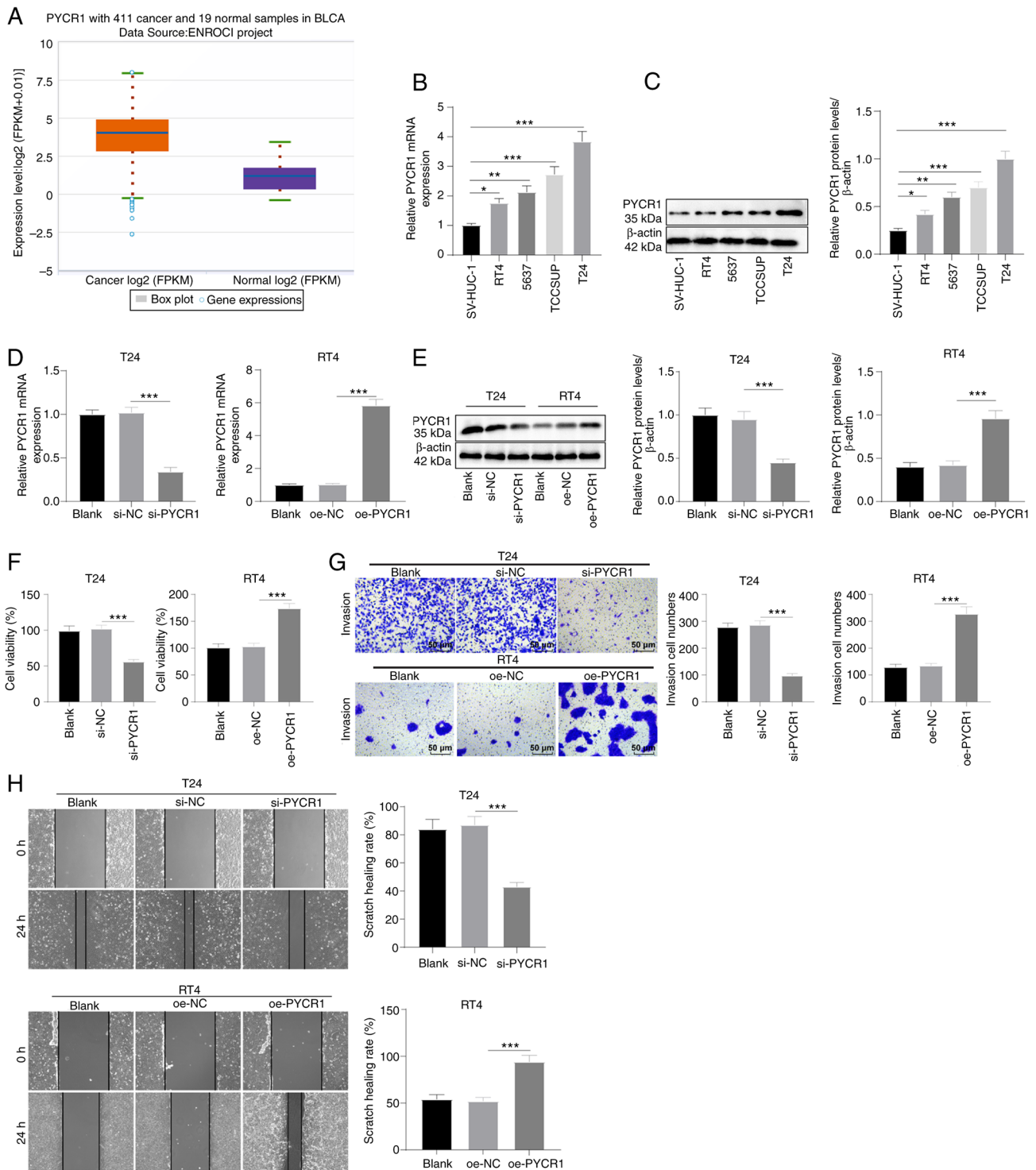
Figure 1. PYCR1 expression is upregulated in BC cells and it promotes cell proliferation, invasion, and migration. (A) Elevated expression of PYCR1 in BC was found by StarBase. (B and C) RT-qPCR and western blot elicited raised mRNA and protein expression levels of PYCR1 in BC cells RT4, 5637, TCCSUP, and T24 relative to normal bladder epithelial cells SV-HUC-1. (D and E) RT-qPCR and western blot manifested repressed mRNA and protein expression levels of PYCR1 in T24 cells after PYCR1 knockout and facilitated levels in RT4 cells after PYCR1 overexpression. (F) MTT assay detected decreased T24 viability and increased RT4 viability. (G) Transwell assay detected reduced T24 invasion and promoted RT4 invasion. (H) Wound-healing assay detected repressed T24 migration and enhanced RT4 migration. Data are presented as the mean ± SD of three repeats. A one-way ANOVA followed by a Tukey's test was used to compare the data. *P<0.05, **P<0.01, ***P<0.001. BC, bladder cancer; PYCR1, pyrroline-5-carboxylate reductase 1; FPKM, Fragments Per Kilobase of exon model per Million mapped fragments; oe, overexpression.

PYCR1 knockdown and increased following PYCR1 over-expression (Fig. 1F, all P<0.001). Transwell wound-healing assays showed that PYCR1 knockdown reduced T24 cell invasion and migration, whereas PYCR1 overexpression stimulated RT4 cell invasion and migration (Fig. 1G and H, all P<0.001). These results confirmed that PYCR1 was highly expressed in BC where it facilitated BC cell proliferation, invasion, and migration.
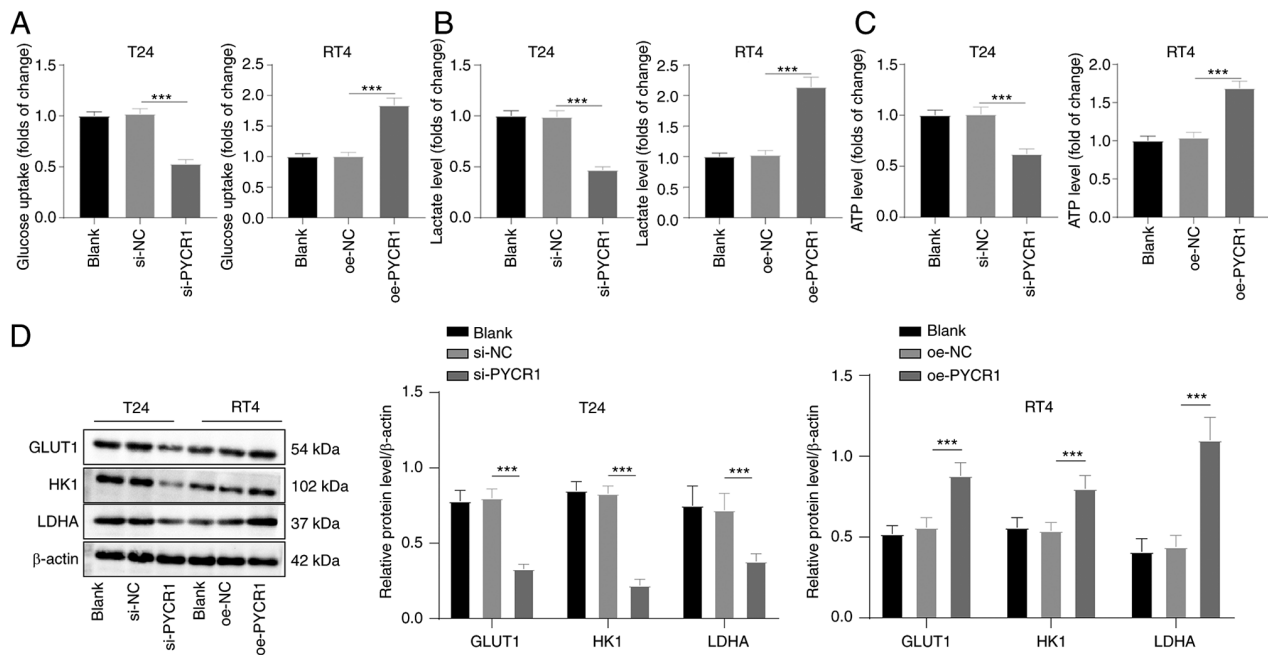
Figure 2. PYCR1 promotes aerobic glycolysis in BC cells. (A-C) Decreased levels of aerobic glycolysis-related-indexes, glucose uptake, lactate production, and ATP production in T24 cells and stimulated levels in RT4 cells. (D) Western blot manifested suppressed expression levels of GLUT1, HK1, and LDHA in T24 cells and amplified expression levels in RT4 cells. Data are presented as the mean ± SD of three repeats. A one-way ANOVA followed by a Tukey's test was used to compare the data. ***$P<0.001$. BC, bladder cancer; PYCR1, pyrroline-5-carboxylate reductase 1; oe, overexpression.

PYCR1 promotes aerobic glycolysis in BC cells. Aerobic glycolysis is important in regulating tumor cell behaviors (33,34). It was speculated that PYCR1 may regulate aerobic glycolysis in BC. The levels of glucose uptake, lactate production, and ATP production in cells after 48 h of transfection were assessed. The levels of glucose uptake, lactate production, and ATP production in T24 cells with PYCR1 expression knocked down were lower, whereas they were increased in RT4 cells overexpressing PYCR1 (Fig. 2A-C, all $P<0.001$). Furthermore, the protein expression levels of aerobic glycolysis-related enzymes GLUT1, HK1, and LDHA were assessed by western blotting. PYCR1 knockdown reduced the protein expression levels of GLUT1, HK1, and LDHA, while PYCR1 overexpression increased the expression levels of these proteins (Fig. 2D, all $P<0.001$). These results suggested that PYCR1 promoted aerobic glycolysis in BC.

PYCR1 promotes activation of the EGFR/PI3K/AKT pathway in BC cells. The EGFR/PI3K/AKT pathway is closely associated with BC cell proliferation, invasion, and metastasis (35) and is implicated in the regulation of aerobic glycolysis (17,18). It was speculated that PYCR1 regulated the EGFR/PI3K/AKT pathway. Western blot assay demonstrated that the EGFR/PI3K/AKT pathway was inhibited, and the p-EGFR/EGFR, p-PI3K/PI3K, and p-AKT/AKT levels were repressed in T24 cells following PYCR1 knockdown, whereas this pathway was activated in RT4 cells following PYCR1 overexpression (Fig. 3A, all $P<0.001$). Thus, PYCR1 activated the EGFR/PI3K/AKT pathway. To probe the mechanism by which PYCR1 regulated the EGFR/PI3K/AKT pathway, the protein-protein interactions between PYCR1 and EGFR were examined by Co-IP, which revealed that endogenous PYCR1 interacted with EGFR protein in T24 cells, suggesting that

PYCR1 could interact with EGFR (Fig. 3B); that is, PYCR1 activated the PI3K/AKT pathway by binding to EGFR.

EGFR pathway inhibitor abrogates the effects of PYCR1 on aerobic glycolysis and BC cell proliferation, invasion, and migration. To confirm that PYCR1 regulated aerobic glycolysis and BC cell growth through the EGFR/PI3K/AKT pathway, RT4 cells overexpressing PYCR1 were treated with the pathway inhibitor CL-387785. Western blotting showed that the EGFR/PI3K/AKT pathway was inhibited by CL-387785, while PYCR1 protein expression was not altered by CL-387785 (Fig. 4A, all $P<0.01$). This result confirmed that EGFR was downstream of PYCR1. Glucose uptake, lactate production, and ATP production levels were also repressed by CL-387785 treatment (Fig. 4B-D, all $P<0.001$), and RT4 cell proliferation, invasion, and migration were also suppressed (Fig. 4E-G; all $P<0.001$). Overall, CL-387785 abrogated the promoting effects of PYCR1 overexpression on aerobic glycolysis and BC cell proliferation, invasion, and migration.

Identification of BMSC-derived Exos and loading of si-PYCR1. MSC-shuttled Exos have a good biological affinity, low toxicity, and low immunogenicity and can be used as carriers to load si-RNA and other drugs to target cancer (20). BMSC-secreted Exos were isolated by differential centrifugation and loaded with si-PYCR1 by electroporation. TEM revealed that Exos were present, visible as the circular saccular body with a double-layer membrane structure and loading si-PYCR1 had no obvious effect on their morphology (Fig. 5A). The particle diameter of the Exos was 54.8±9.6 nm, and the particle size of Exo-si-PYCR1 after loading si-PYCR1 was not changed significantly (Fig. 5B). The potential of Exos was -8.67±0.21 mV, while that of Exo-si-PYCR1 was
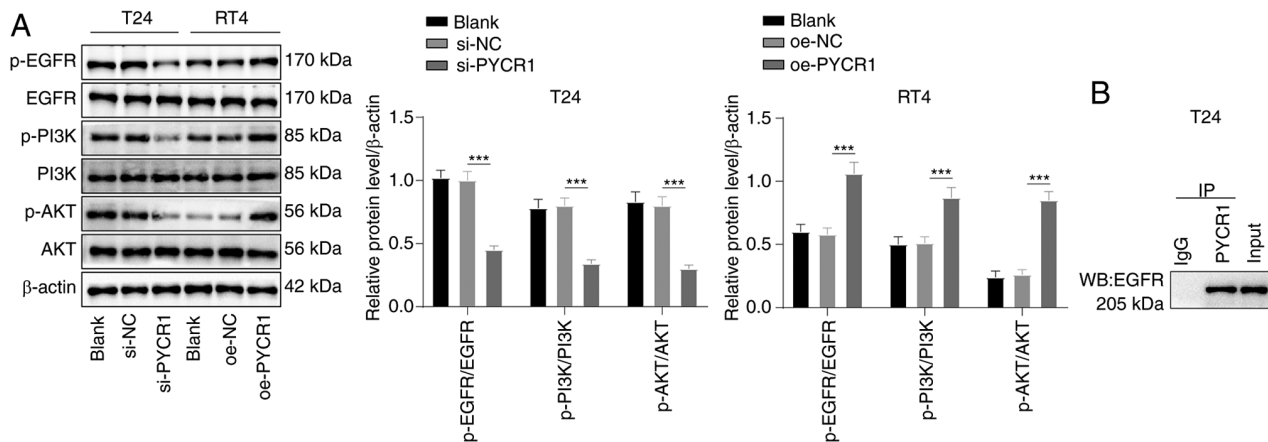
Figure 3. PYCR1 promotes the activation of the EGFR/PI3K/AKT pathway in BC cells. (A) Western blot revealed reduced phosphorylation levels of the EGFR/PI3K/AKT pathway-related proteins in T24 cells and elevated phosphorylation levels in RT4 cells. (B) Co-immunoprecipitation detected protein-protein interactions between endogenous PYCR1 and EGFR in T24 cells. Data are presented as the mean ± SD of three repeats. A one-way ANOVA followed by a Tukey's test was used to compare the data. ***$P<0.001$. BC, bladder cancer; PYCR1, pyrroline-5-carboxylate reductase 1; oe, overexpression.

-14.32±0.18 mV, which indicated that the negatively charged si-PYCR1 was loaded into Exos (Fig. 5C, $P<0.01$). The Exo surface markers CD9, CD81, CD63, and TSG101 in Exos and Exo-si-PYCR1 were positively expressed (Fig. 5D). Agarose gel electrophoresis found that the levels of free si-PYCR1 in Exo-si-PYCR1 were lower, which indicated that si-PYCR1 was loaded into Exos (Fig. 5E). These results indicated that BMSC-shuttled Exos loaded with si-PYCR1 had been successfully obtained.

Exos-si-PYCR1 have stronger inhibitory effects on aerobic glycolysis and proliferation, invasion and migration of BC cells. To evaluate the effects of Exo-si-PYCR1 on BC cells, the proportion of Cy3-labeled Exo-si-PYCR1 entering T24 cells was observed using a laser confocal microscope. The proportion of si-PYCR1 plasmid introduced into T24 cells increased relative to the control group, and the levels of Exo-si-PYCR1 entering the cells was higher in the si-PYCR1 group (Fig. 6A, all $P<0.05$). Exo-si-PYCR1 knocked down PYCR1 levels in T24 cells (Fig. 6B and C, all $P<0.01$). The glucose uptake, lactate production, and ATP production levels were suppressed after Exo-si-PYCR1 treatment, and the inhibitory effect of Exo-si-PYCR1 was more prominent than that of si-PYCR1 transfection (Fig. 6D and F, all $P<0.05$). In addition, Exo-si-PYCR1 inhibited T24 cell proliferation, invasion, and migration, and the inhibitory effect was stronger than that of si-PYCR1 (Fig. 6G-I, all $P<0.05$). Collectively, Exo-si-PYCR1 inhibited aerobic glycolysis and BC cell growth, and the inhibitory effect of Exo-si-PYCR1 was stronger than that of si-PYCR1.

Exo-si-PYCR1 inhibits growth of BC xenograft tumors in nude mice. To validate the inhibitory effects of Exo-si-PYCR1 on BC *in vivo*, T24 cells were injected into nude mice to establish xenograft tumor models of BC. When the volume of the xenograft tumors was ~100 mm³, BMSC-Exos, BMSC-Exo-si-NC, and BMSC-Exo-si-PYCR1 were injected into nude mice through the tail vein. After BMSC-Exo-si-PYCR1 treatment, the PYCR1 levels in tumor tissues were repressed (Fig. 7A and B, all $P<0.001$), and BMSC-Exo-si-PYCR1

inhibited the growth rate, volume, and weight of xenograft tumors in nude mice (Fig. 7C-E, $P<0.001$), and the number of Ki67-positive cells that marked the proliferation of cancer cells in tumor tissues was reduced (Fig. 7F, $P<0.001$), indicating that BMSC-Exo-si-PYCR1 inhibited BC cell proliferation *in vivo*. After the injection of BMSC-Exo-si-PYCR1, any toxic effects of BMSC-Exo, BMSC-Exo-si-NC, and BMSC-Exo-si-PYCR1 were evaluated by observing the changes in the body weight of nude mice and observing any pathological changes in the primary organs (heart, liver, spleen, lung, and kidney) by HE staining. BMSC-Exo, BMSC-Exo-si-NC, and BMSC-Exo-si-PYCR1 had no notable effects on the body weight and the primary organs of nude mice (Fig. 7G-H). These results suggested that the use of BMSC-Exo-si-PYCR1 may be a feasible method for the management of BC.

Discussion

BC is the 4th most prevalent malignancy in men and also a prevalent malignancy in women; it ranges in severity from non-invasive and unaggressive tumors that recur in patients, to long-term invasive surveillance, to invasive and aggressive tumors with high disease-specific mortality (2). Evidence has revealed that upregulation of PYCR1 promotes BC development and progression (36). Exos are important in cell-cell communication that are natural carriers of biological cargo and have become a promising platform for cancer treatment (37). The present study found that si-PYCR1 loaded into BMSC-derived Exos blocked aerobic glycolysis and BC growth via regulation of the EGFR/PI3K/AKT pathway.

The upregulation of PYCR1 contributed to the progression of various cancers such as gastric cancer, nasopharyngeal cancer, and lung cancer (19,38,39). In the present study, it was found that PYCR1 expression was upregulated in BC cells. In particular, the relative expression levels of PYCR1 were highest in T24 cells and lowest in RT4 cells. Therefore, PYCR1 expression was knocked down in T24 cells and overexpressed in RT4 cells to investigate its effects on BC. T24 cells with PYCR1 expression knocked down exhibited reduced viability, invasion, and migration, whereas RT4 cells overexpressing
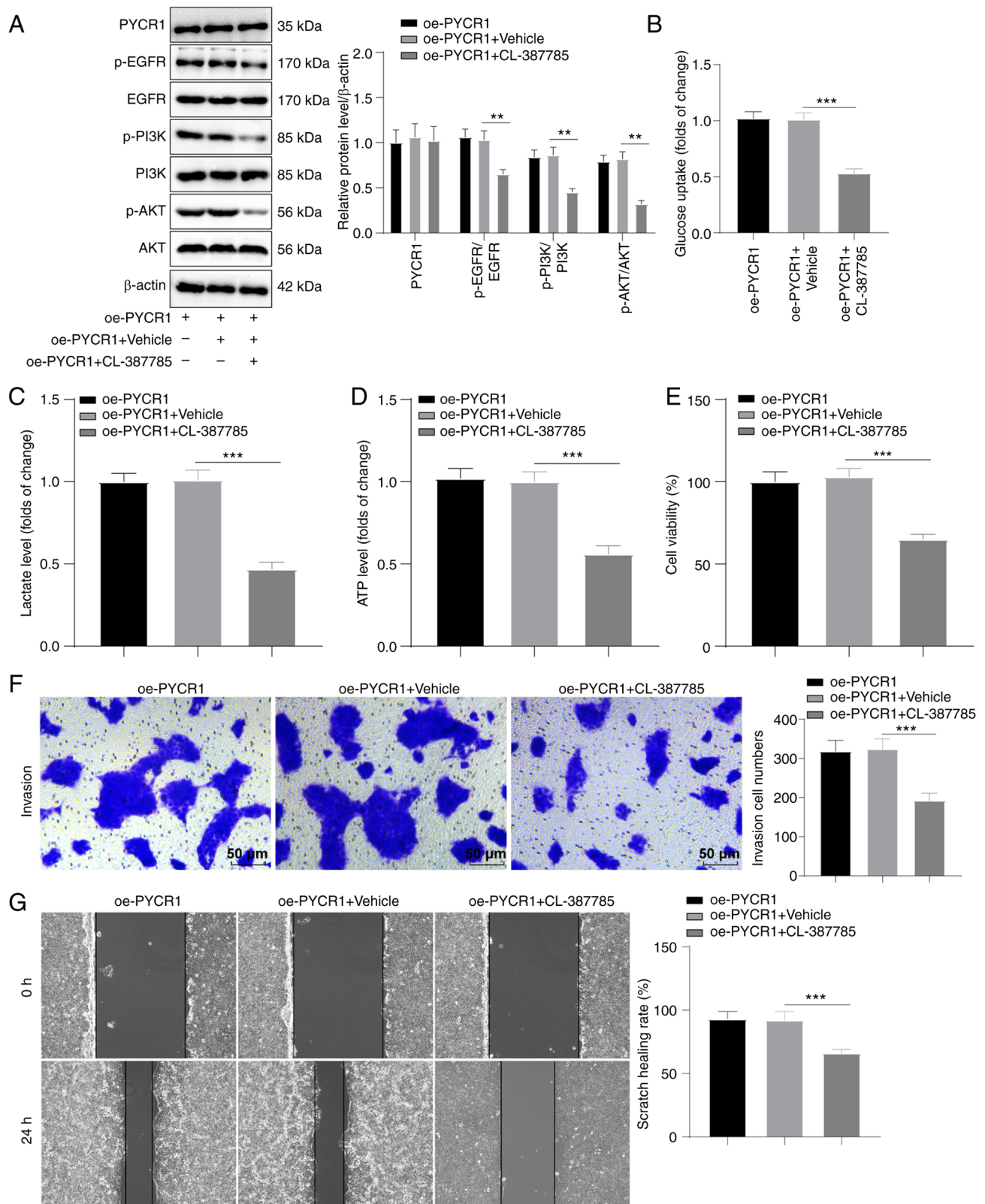
Figure 4. Treatment with an EGFR pathway inhibitor abrogates the effects of PYCR1 on aerobic glycolysis and BC cell proliferation, invasion, and migration. (A) Western blot found no change in protein expression of PYCR1 and repressed phosphorylation levels of the EGFR/PI3K/AKT pathway-related proteins in RT4 cells. (B-D) Colorimetry and reagent kit demonstrated reduced levels of glucose uptake, lactate production, and ATP production in RT4 cells. (E) MTT assay showed weakened RT4 cell viability. (F) Transwell assay manifested limited RT4 cell invasion; G: Scratch test demonstrated blocked RT4 cell migration. Data are presented as the mean ± SD of three repeats. A one-way ANOVA followed by a Tukey's test was used to compare the data. $^{**}P<0.01$, $^{***}P<0.001$. BC, bladder cancer; PYCR1, pyrroline-5-carboxylate reductase 1; oe, overexpression.

PYCR1 exhibited increased viability, invasion, and migration. Consistently, PYCR1 expression was elevated in BC tissues,

and PYCR1 knockdown *in vivo* models resulted in reduced cell growth, whereas PYCR1 overexpression accelerated cell
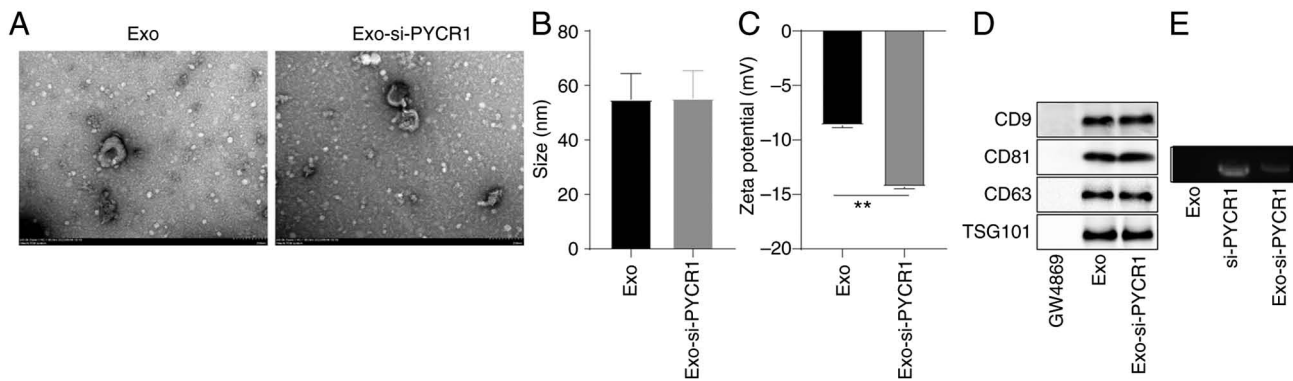
Figure 5. Identification of BMSC-derived Exos and loading of si-PYCR1. (A) The morphological structure of Exos and Exo-si-PYCR1 were double-layered membrane vesicle structure observed using a TEM. (B and C) Particle diameter and potential of Exo and Exo-si-PYCR1 were determined using the particle size analyzer and potential analyzer. (D) The protein expression levels of Exo surface markers CD9, CD63, CD81 and TSG101 were positive, as determined by western blot. GW4869 is the negative control of Exos. (E) The levels of free si-PYCR1 in Exos, si-PYCR1, and Exo-si-PYCR1 were measured by agarose gel electrophoresis (Exo-si-PYCR1 was decreased relative to si-PYCR1). Data are presented as the mean ± SD of three repeats. A one-way ANOVA followed by a Tukey's test was used to compare the data. $^{**}P<0.01$, BMSC, bone marrow-derived stem cell; BC, bladder cancer; PYCR1, pyrroline-5-carboxylate reductase 1; Exo, exosome; si, small interfering; TEM, transmission electron microscopy.

proliferation and invasion (7). In conclusion, high expression of PYCR1 facilitated the proliferation, invasion, and migration of BC cells.

Aerobic glycolysis participates in the regulation of the proliferation, invasion, and migration of various tumor cells including breast cancer, pancreatic cancer, and HCC (9,40,41). Cancer cells must generate sufficient ATP to satisfy the requirements of cell proliferation, and they uptake large quantities of glucose producing high volumes of lactate (42). High glycolytic flux depends on the upregulation of the glycolysis-associated genes (GLUT1, LDHA, and HK1), causing excessive production of lactate (43). Accordingly, it was speculated that PYCR1 might regulate aerobic glycolysis in BC and subsequent examination evidenced that glucose uptake, lactate production, ATP production, and GLUT1, HK1, and LDHA protein levels were suppressed in T24 cells following PYCR1 knockdown, while their levels were increased in RT4 cells following PYCR1 overexpression. PYCR1-dependent proline biosynthesis is critical for tumorigenesis by promoting cell proliferation and linking the proline cycle to glycolysis (44). PYCR1 knockdown induced metabolic transition from glycolysis to oxidative phosphorylation (45). However, there are no reports on the effects of PYCR1 in aerobic glycolysis in BC, to the best of our knowledge. Thus, the present study was the first to show that PYCR1 facilitated aerobic glycolysis in BC.

Downregulation of ring finger protein 126 inhibited the metastasis and proliferation of BC cells through the EGFR/PI3K/AKT pathway (35). The results showed that the EGFR/PI3K/AKT pathway was inhibited and p-EGFR/EGFR, p-PI3K/PI3K, and p-AKT/AKT levels were repressed in T24 cells following PYCR1 knockdown, while the EGFR/PI3K/AKT pathway was activated in RT4 cells overexpressing PYCR1. Previous studies have shown that the EGFR/PI3K/AKT pathway facilitated cancer cell proliferation and suppressed cell apoptosis in various types of cancer (16,46). PYCR1 has been implicated in the regulation of the PI3K/AKT/mTOR axis (19). The results of the present study showed that PYCR1 could interact with EGFR. To further verify the involvement of the EGFR/PI3K/AKT pathway in aerobic glycolysis and

BC growth, RT4 cells overexpressing PYCR1 were treated with the pathway inhibitor CL-387785, and the results showed that CL-387785 inhibited glucose uptake, lactate production, ATP production, and the proliferation, invasion, and migration of RT4 cells, whilst PYCR1 protein expression remained unchanged. Consistently, the PI3K/mTOR pathway inhibitor repressed glycolysis in EGFR-mutant lung adenocarcinoma cells (47). The EGF-like motif is indispensable for VersicanV1 to facilitate aerobic glycolysis in HCC cells and the invasion and metastasis through the activation of the EGFR/PI3K/AKT axis (18). To conclude, CL-387785 abrogated the effects of PYCR1 overexpression on stimulating aerobic glycolysis and BC cell growth.

Owing to their nanometer sizes, Exos have been identified as promising drug delivery tools for the management of cancer (26). si-PYCR1-loaded BMSC-Exos were constructed, and it was found that the levels of Exo-si-PYCR1 entering the cells were elevated. Exos have good biocompatibility and low immunogenicity and can easily be taken up by cells (20,26). The results showed that the number of fluorescent si-PYCR1 plasmids introduced into T24 cells was larger, and thus the inhibitory rate of Exo-si-PYCR1 on PYCR1 expression was higher and the inhibitory effect on aerobic glycolysis and malignant behaviors of T24 cells was more prominent. Exo-si-PYCR1 exerted more prominent effects on suppressing PYCR1 levels, inhibiting glucose uptake, lactate production, and ATP production, and preventing the proliferation, invasion and migration of T24 cells than si-PYCR1, illustrating for the first time that Exo-si-PYCR1 suppressed aerobic glycolysis and BC cell growth, and the inhibitory effect of Exo-si-PYCR1 was stronger than that of si-PYCR1. The in vivo results showed that BMSC-Exo-si-PYCR1 repressed xenograft tumor growth in nude mice and decreased BC cell proliferation. In addition, BMSC-Exo-si-PYCR1 had no obvious effect on the primary organs and body weight of nude mice. In conclusion, loading Exos with si-PYCR1 to knock down PYCR1 in cancerous cells specifically may serve as a feasible method to treat BC.

In summary, this study showed for the first time that PYCR1 regulated aerobic glycolysis and BC cell growth via
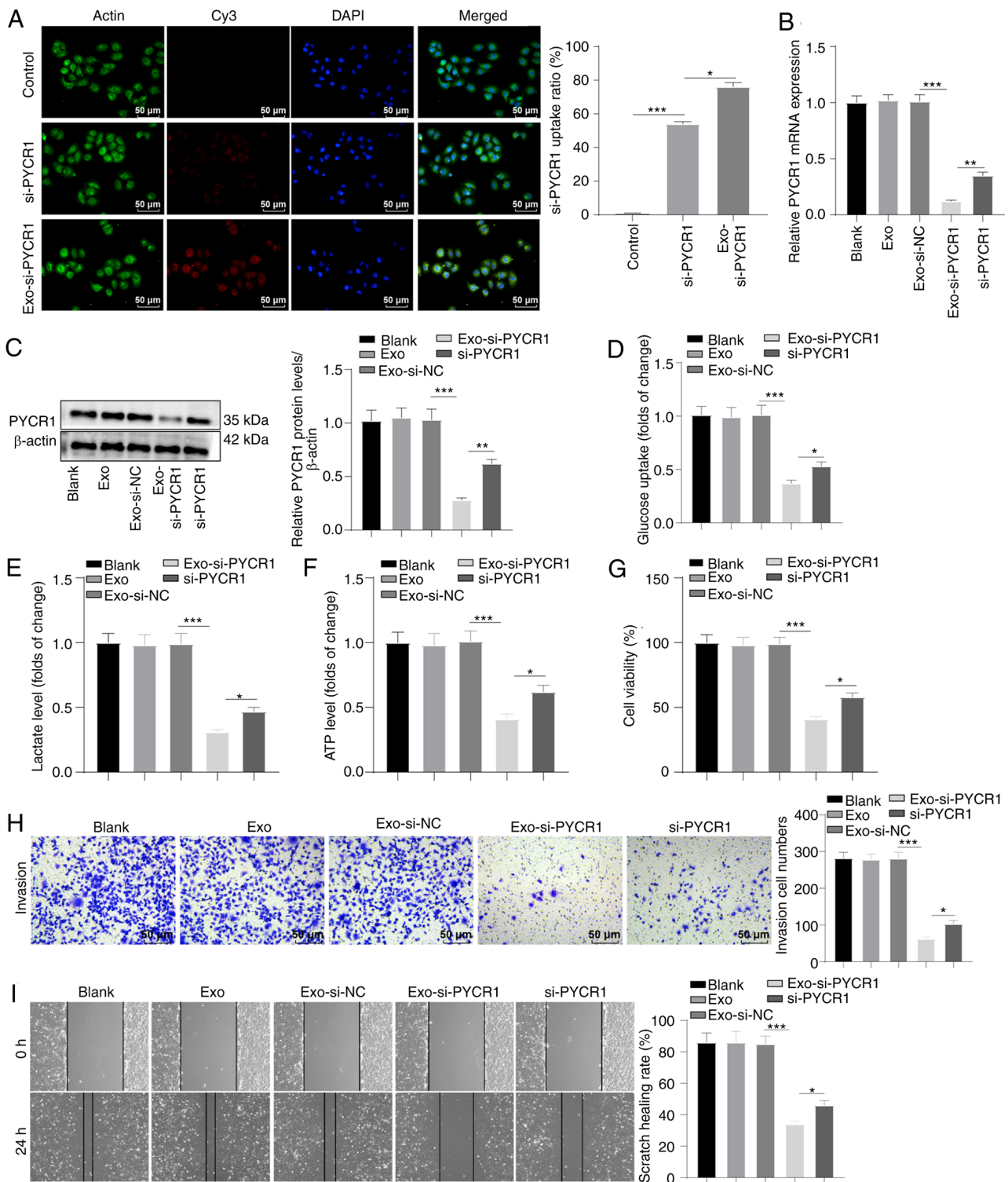
Figure 6. Exo-si-PYCR1 has a stronger inhibitory effect on aerobic glycolysis and BC cell proliferation, invasion, and migration. (A) The uptake of Cy3-labeled si-PYCR1 by T24 cells was observed using laser confocal microscopy. (B and C) RT-qPCR and western blot revealed reduced mRNA and protein expression levels of PYCR1 in Exo-si-PYCR1-treated T24 cells. (D-F) Colorimetry and reagent kit demonstrated diminished levels of glucose uptake, lactate production, and ATP production in Exo-si-PYCR1-treated T24 cells. (G) MTT assay detected blocked proliferation in Exo-si-PYCR1-treated T24 cells. (H) Transwell assays detected weakened invasion in Exo-si-PYCR1-treated T24 cells. (I) Wound-healing assay detected suppressed migration in Exo-si-PYCR1-treated T24 cells. Data are presented as the mean ± SD of three repeats. A one-way ANOVA followed by a Tukey's test was used to compare the data. $^{*}P<0.05$, $^{**}P<0.01$, $^{***}P<0.001$. BC, bladder cancer; PYCR1, pyrroline-5-carboxylate reductase 1; Exo, exosome; si, small interfering.

the EGFR/PI3K/AKT pathway. Furthermore, Exo-si-PYCR1 was constructed, a nano nucleic acid drug with BMSC-Exos as its carrier and verified that they inhibited BC progression through *in vivo* and *in vitro* experiments, serving as a reference

for the development of Exo-targeted therapeutic drugs for BC and other types of cancer. However, there was no further in-depth study on the binding sites and intermolecular interactions between PYCR1 and EGFR, or the regulatory effects of
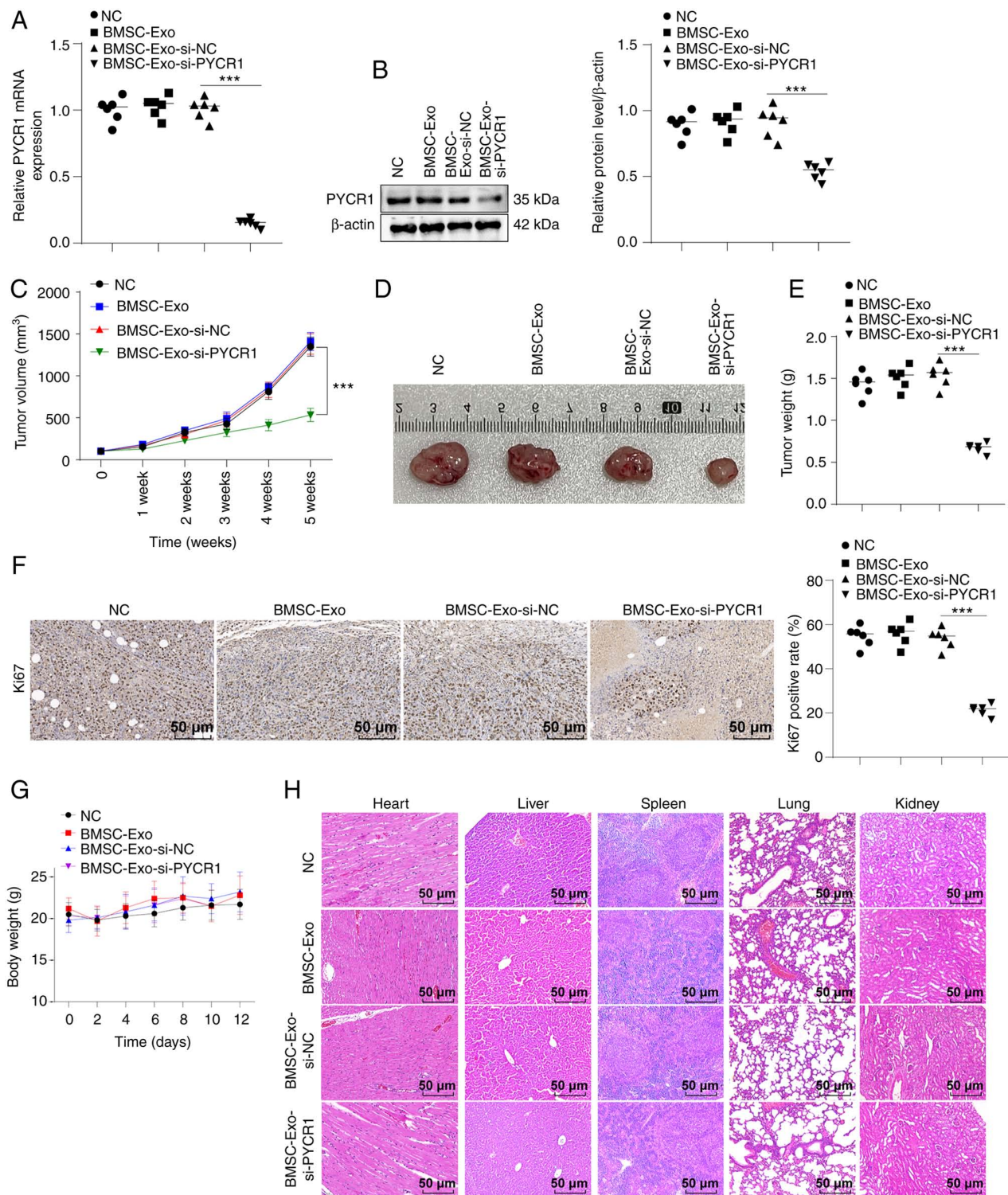
Figure 7. Exo-si-PYCR1 prevents BC xenograft tumor growth in nude mice and exhibits good biological safety. T24 cells were subcutaneously injected into nude mice to establish a tumor model of BC. When the tumor volume grew to ~100 mm^3, BMSC-Exo, BMSC-Exo-si-NC, or BMSC-Exo-si-PYCR1 was injected into mice through the tail vein. The NC group was injected with an equivalent volume of normal saline. (A and B) RT-qPCR and western blot demonstrated decreased mRNA and protein expression levels of PYCR1 in tumor tissues of the BMSC-Exo-si-PYCR1 group. (C) The volume of the xenograft tumor in nude mice of the BMSC-Exo-si-PYCR1 was decreased. (D) The size of the xenograft tumor. (E) The weight of the xenograft tumor in the BMSC-Exo-si-PYCR1 group was reduced. (F) The percentage of Ki67-positive cells in tumor tissues was determined by immunohistochemistry. (G) The body weight of nude mice 12 days after administration maintained stability. (H) There were no obvious changes in cell morphology of the heart, liver, spleen, lung, and kidney of nude mice analyzed by HE staining. n=6 mice/group. Data are presented as the mean ± SD of three repeats. A Student's t-test or a one-way ANOVA followed by a Tukey's test was used to compare the data. ***P<0.001. BC, bladder cancer; PYCR1, pyrroline-5-carboxylate reductase 1; Exo, exosome; si, small interfering; BMSC, bone marrow-derived stem cell; Exo, exosome; NC, negative control; HE, hematoxylin and eosin.

PYCR1 on the EGFR/PI3K/AKT pathway in animal experiments. In addition, the therapeutic efficacy and biosafety of

Exo-si-PYCR1 need to be verified through larger animal experiments. The regulatory role of PYCR1 in regulating the

EGRF/PI3K/AKT pathway and glycolysis in BC cells was confirmed using both knockdown and overexpression experiments with RT4 and T24 cells. In the preliminary experiments, PYCR1 was overexpressed in RT4 cells and knocked down in T24 cells, and the results showed that PYCR1 overexpression could activate the EGFR/PI3K/AKT pathway. To validate whether PYCR1 regulates aerobic glycolysis and the growth of bladder cancer cells through the EGFR/PI3K/AKT pathway, the EGFR inhibitor CL-387785 was used to treat RT4 cells overexpressing PYCR1 in rescue experiments. Therefore, RT4 cells were selected for the functional experiments. It is hypothesized that the difference between the two cell types will have little impact on the present experimental results. Moreover, the overall experimental design was relatively complete. In the future, these limitations will be addressed. Furthermore, the molecular mechanism of the regulatory effects of PYCR1/EGFR/PI3K/AKT using animal experiments will be assessed to further verify the therapeutic effect and biosafety of Exo-si-PYCR1 and develop and construct additional nanonucleic acid drugs based on tumor therapeutic drugs and key factors associated with targeted inhibition of tumor progression through siRNAs to efficiently target tumors.

Availability of data and materials

The datasets used and/or analyzed during the present study are available from the corresponding author on reasonable request.

Authors' contributions

WS is the guarantor of integrity of the entire study. ZL and WS conceived the study. YWL designed the study and was involved in data acquisition. YJ performed the literature research. JL contributed to the manuscript preparation. WS and ZL wrote and edited the manuscript. HFF and YJ performed the experiments. HFF, JL and QY performed the data analysis. ZL and YWL confirm the authenticity of all the raw data. All authors have read and approved the final manuscript.

Ethics approval and consent to participate

All procedures were authorized by the Academic Ethics Committee of Hunan Provincial People's Hospital, The First Affiliated Hospital of Hunan Normal University (approval no. 2021-071) and were strictly implemented in accordance with the National Laboratory Animal Guide. Laboratory procedures were performed in such a manner as to reduce the pain and discomfort caused to mice.

Patient consent for publication

Not applicable.

Competing interests

The authors declare that they have no competing interests.

References

1. Dobruch J and Oszczudlowski M: Bladder cancer: Current challenges and future directions. Medicina (Kaunas) 57: 749, 2021.
2. Lenis AT, Lec PM, Chamie K and Mshs MD: Bladder cancer: A review. JAMA 324: 1980-1991, 2020.
3. Siracusano S, Rizzetto R and Porcaro AB: Bladder cancer genomics. Urologia 87: 49-56, 2020.
4. Na L, Wang Z, Bai Y, Sun Y, Dong D, Wang W and Zhao C: WNT7B represses epithelial-mesenchymal transition and stem-like properties in bladder urothelial carcinoma. Biochim Biophys Acta Mol Basis Dis 1868: 166271, 2022.
5. Hollinshead KER, Munford H, Eales KL, Bardella C, Li C, Escribano-Gonzalez C, Thakker A, Nonnenmacher Y, Kluckova K, Jeeves M, et al: Oncogenic IDH1 mutations promote enhanced proline synthesis through PYCR1 to support the maintenance of mitochondrial redox homeostasis. Cell Rep 22: 3107-3114, 2018.
6. Westbrook RL, Bridges E, Roberts J, Escribano-Gonzalez C, Eales KL, Vettore LA, Walker PD, Vera-Siguenza E, Rana H, Cuozzo F, et al: Proline synthesis through PYCR1 is required to support cancer cell proliferation and survival in oxygen-limiting conditions. Cell Rep 38: 110320, 2022.
7. Du S, Sui Y, Ren W, Zhou J and Du C: PYCR1 promotes bladder cancer by affecting the Akt/Wnt/beta-catenin signaling. J Bioenerg Biomembr 53: 247-258, 2021.
8. El-Far AH, Al Jaouni SK, Li X and Fu J: Cancer metabolism control by natural products: Pyruvate kinase M2 targeting therapeutics. Phytother Res 36: 3181-3201, 2022.
9. Wu Z, Wu J, Zhao Q, Fu S and Jin J: Emerging roles of aerobic glycolysis in breast cancer. Clin Transl Oncol 22: 631-646, 2020.
10. Hua S, Lei L, Deng L, Weng X, Liu C, Qi X, Wang S, Zhang D, Zou X, Cao C, et al: miR-139-5p inhibits aerobic glycolysis, cell proliferation, migration, and invasion in hepatocellular carcinoma via a reciprocal regulatory interaction with ETS1. Oncogene 37: 1624-1636, 2018.
11. Ji H, Li D, Chen L, Shimamura T, Kobayashi S, McNamara K, Mahmood U, Mitchell A, Sun Y, Al-Hashem R, et al: The impact of human EGFR kinase domain mutations on lung tumorigenesis and in vivo sensitivity to EGFR-targeted therapies. Cancer Cell 9: 485-495, 2006.
12. Jamal-Hanjani M, Wilson GA, McGranahan N, Birkbak NJ, Watkins TBK, Veeriah S, Shafi S, Johnson DH, Mitter R, Rosenthal R, et al: Tracking the evolution of non-small-cell lung cancer. N Engl J Med 376: 2109-2121, 2017.
13. Mertins P, Mani DR, Ruggles KV, Gillette MA, Clauser KR, Wang P, Wang X, Qiao JW, Cao S, Petralia F, et al: Proteogenomics connects somatic mutations to signalling in breast cancer. Nature 534: 55-62, 2016.
14. Srivatsa S, Paul MC, Cardone C, Holcmann M, Amberg N, Pathria P, Diamanti MA, Linder M, Timelthaler G, Dienes HP, et al: EGFR in tumor-associated myeloid cells promotes development of colorectal cancer in mice and associates with outcomes of patients. Gastroenterology 153: 178-190 e110, 2017.
15. Sun C, Wang L, Huang S, Heynen GJJE, Prahallad A, Robert C, Haanen J, Blank C, Wesseling J, Willems SM, et al: Reversible and adaptive resistance to BRAF(V600E) inhibition in melanoma. Nature 508: 118-122, 2014.
16. Zhang B, Zhang Y, Jiang X, Su H, Wang Q, Wudu M, Jiang J, Ren H, Xu Y, Liu Z and Qiu X: JMJD8 promotes malignant progression of lung cancer by maintaining EGFR stability and EGFR/PI3K/AKT pathway activation. J Cancer 12: 976-987, 2021.
17. Lee JH, Liu R, Li J, Wang Y, Tan L, Li XJ, Qian X, Zhang C, Xia Y, Xu D, et al: EGFR-phosphorylated platelet isoform of phosphofructokinase 1 promotes PI3K activation. Mol Cell 70: 197-210 e197, 2018.

18. Zhangyuan G, Wang F, Zhang H, Jiang R, Tao X, Yu D, Jin K, Yu W, Liu Y, Yin Y, *et al*: VersicanV1 promotes proliferation and metastasis of hepatocellular carcinoma through the activation of EGFR-PI3K-AKT pathway. Oncogene 39: 1213-1230, 2020.

19. Xiao S, Li S, Yuan Z and Zhou L: Pyrroline-5-carboxylate reductase 1 (PYCR1) upregulation contributes to gastric cancer progression and indicates poor survival outcome. Ann Transl Med 8: 937, 2020.

20. Jiang X, Fu J, Zhong J, Li X, Wang H, Zhong S, Wei Y, Zhao X, Chen X, Zhou Y, *et al*: Guanidinylated cyclic synthetic polypeptides can effectively deliver siRNA by mimicking the biofunctions of both cell-penetrating peptides and nuclear localization signal peptides. ACS Macro Lett 10: 767-773, 2021.

21. Gabrielson NP, Lu H, Yin L, Kim KH and Cheng J: A cell-penetrating helical polymer for siRNA delivery to mammalian cells. Mol Ther 20: 1599-1609, 2012.

22. Singh A, Trivedi P and Jain NK: Advances in siRNA delivery in cancer therapy. Artif Cells Nanomed Biotechnol 46: 274-283, 2018.

23. Song Z, Han Z, Lv S, Chen C, Chen L, Yin L and Cheng J: Synthetic polypeptides: from polymer design to supramolecular assembly and biomedical application. Chem Soc Rev 46: 6570-6599, 2017.

24. Liao W, Du Y, Zhang C, Pan F, Yao Y, Zhang T and Peng Q: Exosomes: The next generation of endogenous nanomaterials for advanced drug delivery and therapy. Acta Biomater 86: 1-14, 2019.

25. Zhang L and Yu D: Exosomes in cancer development, metastasis, and immunity. Biochim Biophys Acta Rev Cancer 1871: 455-468, 2019.

26. Zhang Y, Liu Q, Zhang X, Huang H, Tang S, Chai Y, Xu Z, Li M, Chen X, Liu J, *et al*: Recent advances in exosome-mediated nucleic acid delivery for cancer therapy. J Nanobiotechnology 20: 279, 2022.

27. National Standard of the P.R.C GB/T 39760-2021 Laboratory animal Guidelines for euthanasia.

28. Song X, Xue Y, Fan S, Hao J and Deng R: Lipopolysaccharide-activated macrophages regulate the osteogenic differentiation of bone marrow mesenchymal stem cells through exosomes. PeerJ 10: e13442, 2022.

29. Livak KJ and Schmittgen TD: Analysis of relative gene expression data using real-time quantitative PCR and the 2(-Delta Delta C(T)) method. Methods 25: 402-408, 2001.

30. Hira VVV, de Jong AL, Ferro K, Khurshed M, Molenaar RJ and Van Noorden CJF: Comparison of different methodologies and cryostat versus paraffin sections for chromogenic immunohistochemistry. Acta Histochem 121: 125-134, 2019.

31. Cheng C, Song D, Wu Y and Liu B: RAC3 promotes proliferation, migration and invasion via PYCR1/JAK/STAT signaling in bladder cancer. Front Mol Biosci 7: 218, 2020.

32. Liu Z, Sun T, Zhang Z, Bi J and Kong C: An 18-gene signature based on glucose metabolism and DNA methylation improves prognostic prediction for urinary bladder cancer. Genomics 113: 896-907, 2021.

33. Cao L, Wu J, Qu X, Sheng J, Cui M, Liu S, Huang X, Xiang Y, Li B, Zhang X and Cui R: Glycometabolic rearrangements-aerobic glycolysis in pancreatic cancer: Causes, characteristics and clinical applications. J Exp Clin Cancer Res 39: 267, 2020.

34. Gentric G, Mieulet V and Mechta-Grigoriou F: Heterogeneity in cancer metabolism: New concepts in an old field. Antioxid Redox Signal 26: 462-485, 2017.

35. Xu H, Ju L, Xiong Y, Yu M, Zhou F, Qian K, Wang G, Xiao Y and Wang X: E3 ubiquitin ligase RNF126 affects bladder cancer progression through regulation of PTEN stability. Cell Death Dis 12: 239, 2021.

36. Song W, Yang K, Luo J, Gao Z and Gao Y: Dysregulation of USP18/FTO/PYCR1 signaling network promotes bladder cancer development and progression. Aging (Albany NY) 13: 3909-3925, 2021.

37. Arrighetti N, Corbo C, Evangelopoulos M, Pasto A, Zuco V and Tasciotti E: Exosome-like nanovectors for drug delivery in cancer. Curr Med Chem 26: 6132-6148, 2019.

38. Li Z, Zhou X, Huang J, Xu Z, Xing C, Yang J and Zhou X: MicroRNA hsa-miR-150-5p inhibits nasopharyngeal carcinogenesis by suppressing PYCR1 (pyrroline-5-carboxylate reductase 1). Bioengineered 12: 9766-9778, 2021.

39. Sang S, Zhang C and Shan J: Pyrroline-5-carboxylate reductase 1 accelerates the migration and invasion of nonsmall cell lung cancer in vitro. Cancer Biother Radiopharm 34: 380-387, 2019.

40. Feng J, Li J, Wu L, Yu Q, Ji J, Wu J, Dai W and Guo C: Emerging roles and the regulation of aerobic glycolysis in hepatocellular carcinoma. J Exp Clin Cancer Res 39: 126, 2020.

41. Hu Q, Qin Y, Ji S, Xu W, Liu W, Sun Q, Zhang Z, Liu M, Ni Q, Yu X and Xu X: UHRF1 promotes aerobic glycolysis and proliferation via suppression of SIRT4 in pancreatic cancer. Cancer Lett 452: 226-236, 2019.

42. de la Cruz-Lopez KG, Castro-Munoz LJ, Reyes-Hernandez DO, Garcia-Carranca A and Manzo-Merino J: Lactate in the regulation of tumor microenvironment and therapeutic approaches. Front Oncol 9: 1143, 2019.

43. Massari F, Ciccarese C, Santoni M, Iacovelli R, Mazzucchelli R, Piva F, Scarpelli M, Berardi R, Tortora G, Lopez-Beltran A, *et al*: Metabolic phenotype of bladder cancer. Cancer Treat Rev 45: 46-57, 2016.

44. Liu W, Hancock CN, Fischer JW, Harman M and Phang JM: Proline biosynthesis augments tumor cell growth and aerobic glycolysis: Involvement of pyridine nucleotides. Sci Rep 5: 17206, 2015.

45. Tejedor G, Contreras-Lopez R, Barthelaix A, Ruiz M, Noël D, Ceuninck FD, Pastoureau P, Luz-Crawford P, Jorgensen C and Djouad F: Pyrroline-5-carboxylate reductase 1 directs the cartilage protective and regenerative potential of murphy roths large mouse mesenchymal stem cells. Front Cell Dev Biol 9: 604756, 2021.

46. Wang Y, Wang C, Fu Z, Zhang S and Chen J: miR-30b-5p inhibits proliferation, invasion, and migration of papillary thyroid cancer by targeting GALNT7 via the EGFR/PI3K/AKT pathway. Cancer Cell Int 21: 618, 2021.

47. Makinoshima H, Takita M, Saruwatari K, Umemura S, Obata Y, Ishii G, Matsumoto S, Sugiyama E, Ochiai A, Abe R, *et al*: Signaling through the phosphatidylinositol 3-kinase (PI3K)/mammalian target of rapamycin (mTOR) axis is responsible for aerobic glycolysis mediated by glucose transporter in epidermal growth factor receptor (EGFR)-mutated lung adenocarcinoma. J Biol Chem 290: 17495-17504, 2015.